Environmental Science & Technology

Article

pubs.acs.org/est

Response of Global Particulate-Matter-Related Mortality to Changes in Local Precursor Emissions

Colin J. Lee,*[,†] Randall V. Martin,[†,‡] Daven K. Henze,[§] Michael Brauer,[∥] Aaron Cohen,[⊥] and Aaron van Donkelaar[†]

[†]Dalhousie University, Halifax, Nova Scotia B3H 4R2, Canada

[‡]Harvard−Smithsonian Center for Astrophysics, Cambridge, Massachusetts 02138, United States

[§]University of Colorado, Boulder, Colorado 80309, United States

[∥]School of Population and Public Health, University of British Columbia, Vancouver, British Columbia V6T 1Z4, Canada

[⊥]Health Effects Institute, Boston, Massachusetts 02110-1817, United States

Supporting Information

ABSTRACT: Recent Global Burden of Disease (GBD) assessments estimated that outdoor fine-particulate matter ($PM_{2.5}$) is a causal factor in over 5% of global premature deaths. $PM_{2.5}$ is produced by a variety of direct and indirect, natural and anthropogenic processes that complicate $PM_{2.5}$ management. This study develops a proof-of-concept method to quantify the effects on global premature mortality of changes to $PM_{2.5}$ precursor emissions. Using the adjoint of the GEOS-Chem chemical transport model, we calculated sensitivities of global $PM_{2.5}$-related premature mortality to emissions of precursor gases (SO_2, NO_x, NH_3) and carbonaceous aerosols. We used a satellite-derived ground-level $PM_{2.5}$ data set at approximately 10 × 10 km^2 resolution to better align the exposure with population density. We used exposure-response functions from the GBD project to relate mortality to exposure in the adjoint calculation. The response of global mortality to changes in local anthropogenic emissions varied spatially by several orders of magnitude. The largest reductions in mortality for a 1 kg km^{-2} yr^{-1} decrease in emissions were for ammonia and carbonaceous aerosols in Eastern Europe. The greatest reductions in mortality for a 10% decrease in emissions were found for secondary inorganic sources in East Asia. In general, a 10% decrease in SO_2 emissions was the most effective source to control, but regional exceptions were found.

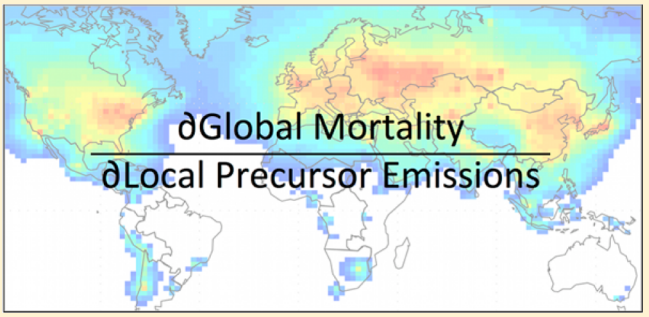

INTRODUCTION

Long-term exposure to fine particulate matter with an aerodynamic diameter less than 2.5 μm ($PM_{2.5}$) is associated with morbidity and mortality.[1,2] $PM_{2.5}$ can be produced directly by combustion or mechanical processes, and indirectly by condensation of aerosol precursor gases. The Global Burden of Disease (GBD) project estimated that exposure to ambient $PM_{2.5}$ contributed to 3.2 million (5% of the global total) premature deaths worldwide in 2010.[3] Emission control strategies can be costly, and the pathways from emissions to exposure are complex.[4−6] It is, therefore, important to determine how future changes in $PM_{2.5}$ sources would affect health outcomes.

A variety of techniques have been employed to estimate the impacts of emissions on the attributable fraction of mortality due to $PM_{2.5}$ exposure.[7] In general, exposure is estimated at some baseline and compared with exposure estimated after a perturbation in emissions. This comparison can be based on measured concentrations before and after a natural experiment such as the strict air-quality controls enacted for the 2008 Beijing Olympics,[8−10] or the U.S. Clean Air Act.[11,12] These types of studies are limited by the regional scope of the policy.

Alternatively, a chemical transport model can be used to calculate atmospheric concentrations based on different emissions scenarios. For example, Anenberg et al.[13] used two model simulations, one with modern emissions and one with preindustrial emissions, to estimate the additional burden of disease produced by modern emissions for the whole world. West et al.[14] perturbed NO_x emissions separately in each of nine global regions to determine regional impacts on global O_3 exposure, while Anenberg et al.[15] similarly perturbed ozone precursor emissions together in each of five global regions. Similar methods have been used to test other specific scenarios.[16,17] While this approach has provided valuable insights, it can be computationally prohibitive to examine more than a few specific circumstances. Adjoint models allow for the simultaneous computation of an entire field (e.g., >

Received: September 3, 2014
Accepted: March 2, 2015
Published: March 2, 2015

DOI: 10.1021/acs.est.5b00873
Environ. Sci. Technol. 2015, 49, 4335−4344

10 000) of responses and thus explore novel policy-relevant questions. The recent development of the adjoint of a global chemical transport model to include aerosols[18] offers an exciting opportunity to efficiently determine the responses of global mortality to changes in local emissions.

In adjoint modeling, a change in the final state is transformed backward in time to determine the sensitivities of the final state to model inputs, such as emissions. Recently, adjoint chemical transport models have been used to constrain estimates of sources of $PM_{2.5}$.[19−22] Pappin and Hakami[23] used the gas-phase chemistry adjoint of a regional model (CMAQ) to determine the benefits of reducing emissions that contribute to trace-gas air pollutant exposure in Canada and the United States, demonstrating the utility of this novel tool in health-impact studies.

The relationship between gaseous emissions and $PM_{2.5}$ concentrations is complex. The main species that result in secondary formation of inorganic $PM_{2.5}$ are sulfur dioxide (SO_2), nitrogen oxides (NO_x = NO + NO_2) and ammonia (NH_3). In the atmosphere, SO_2 is rapidly oxidized to form sulfuric acid (H_2SO_4), which readily condenses to form sulfate (SO_4^{2-}) $PM_{2.5}$. NO_x is oxidized to nitric acid (HNO_3), which can exist in the gas phase. NH_3 preferentially reacts with H_2SO_4 and remaining NH_3 will react with HNO_3 to form ammonium nitrate (NH_4NO_3) particles. The relationship between any one of the precursor gases and $PM_{2.5}$ concentrations is therefore a function of the concentrations of the others. Furthermore, secondary inorganic aerosols are part of a complex mixture of other $PM_{2.5}$ components, some of which are more readily modifiable (e.g., primary carbonaceous) than others (e.g., mineral dust, sea salt). Over the past decade SO_2 and NO_x emissions as well as $PM_{2.5}$ concentrations have decreased in North America and Europe, in contrast with increases in South Asia and East Asia.[20,24−26] Globally, NH_3 emissions are more uncertain and generally increasing.[27−29]

Here, we introduce and evaluate the capability to determine the response of global $PM_{2.5}$-related mortality to local changes in inorganic $PM_{2.5}$ precursor gases and primary carbonaceous emissions through use of a full (gas- and particulate-phase) adjoint model.

METHODS

To calculate responses of global premature mortality to changes in $PM_{2.5}$ sources, we employed the GEOS-Chem global chemical transport model[30,31] and its adjoint.[18] We included information from a satellite-derived $PM_{2.5}$ climatology[32] to improve the accuracy and spatial resolution of the model exposure, as described below. We then calculated global premature mortality at the country level based on the exposure-response relationship of the GBD project as presented by Burnett et al.[33]

Estimation of Exposure by Satellite Remote Sensing. Adjoint modeling requires an initial estimate from which to calculate responses. The initial ambient $PM_{2.5}$ concentrations were obtained from satellite remote sensing and modeling.

Model spatial resolution has been shown to have a significant effect on predicted health outcomes; Punger and West[34] found a 30% difference in premature mortality due to $PM_{2.5}$ exposure calculated at 200 km resolution compared with 12 km resolution. Satellite remote sensing offers global observational information about $PM_{2.5}$ through measurement of aerosol optical depth (AOD). Van Donkelaar et al.[32] produced a long-term (2001−2006) global surface $PM_{2.5}$ data set at a resolution of 0.1° × 0.1° (~10 × 10 km^2), by combining satellite AOD measurements with knowledge of the relationship between surface $PM_{2.5}$ and AOD from GEOS-Chem simulations and found that these data well represented $PM_{2.5}$ monitors in North America (r = 0.77, slope = 1.07, n = 1057) and elsewhere in the world (r = 0.83, slope = 0.86, n = 244). These data were used, along with surface measurements and chemical transport model estimates, in the GBD project as described by Brauer et al.[35] We similarly used this information here. Supporting Information (SI) Table S-1 quantifies how the spatial resolution of the $PM_{2.5}$ concentrations affects exposure. We further scaled these satellite values by 1.16 to account for their overall bias versus global ground-based $PM_{2.5}$ monitors as found by van Donkelaar et al.[32] We then turn to a chemical transport model (GEOS-Chem; www.geos-chem.org) to temporally distribute the satellite-derived $PM_{2.5}$ data set to be consistent with the processes used in the adjoint model. The GEOS-Chem simulation solves for atmospheric transport and chemistry of 72 chemical families, including $PM_{2.5}$ precursors such as SO_2, NH_3, and NO_x, based on emissions and assimilated meteorology; a full description of the simulation is available in SI section S-2 and is evaluated in SI section S-3. Emissions are in SI Table S-2. We focused on the year 2005 for which mortality and satellite data were readily available.

Adjoint Modeling to Relate Mortality to $PM_{2.5}$ Sources. We used the adjoint of GEOS-Chem to determine the response of global $PM_{2.5}$-related mortality to changes in emissions of carbonaceous particles and inorganic precursor gases that form a large portion of ambient $PM_{2.5}$. The GEOS-Chem adjoint[18] allows for efficient computation of the partial derivatives of some scalar-valued function of the model output, the cost function, with respect to input conditions. In this work, we extended the GEOS-Chem adjoint to include calculation of sensitivity of global mortality to $PM_{2.5}$ precursor emissions. We defined a cost function (SI section S-5) as the total global premature mortality based on average ambient $PM_{2.5}$ concentrations as described in the previous section. Then we used the adjoint model to calculate for the entire year the field of partial derivatives of this cost function with respect to the modeled atmospheric state at each time step in each model grid box, which we refer to as the adjoint forcing. The adjoint evolves these forcings chemically and through transport backward in time toward emissions. The outputs provided by the adjoint, the sensitivities, are the partial derivatives of the cost function with respect to emissions in each location. In this way, it can be said that the adjoint method is a receptor-oriented approach, which calculates the regionally distributed influences on a single outcome. After computing the model sensitivities, we multiplied the field by a constant change in emissions (either 1 kg km^{-2} yr^{-1} or 10%), to provide the model response of global $PM_{2.5}$-related mortality to a change (increase or decrease) in emissions. We refer to the responses in each location (a single 2° × 2.5° GEOS-Chem grid box) as local responses to differentiate them from regional responses aggregated over multiple grid boxes.

For this study, we calculated responses to absolute changes in NH_3, SO_2, and NO_x (inorganic precursor gases), as well as primary carbonaceous aerosols of organic matter (OM) and black carbon (BC). We considered responses to relative changes in emissions of precursor gases from mainly land-based human activities and primary carbonaceous aerosols from combustion of fossil fuels, open biomass burning and biofuel burning. We focused on these sources because they comprise

DOI: 10.1021/acs.est.5b00873
Environ. Sci. Technol. 2015, 49, 4335−4344

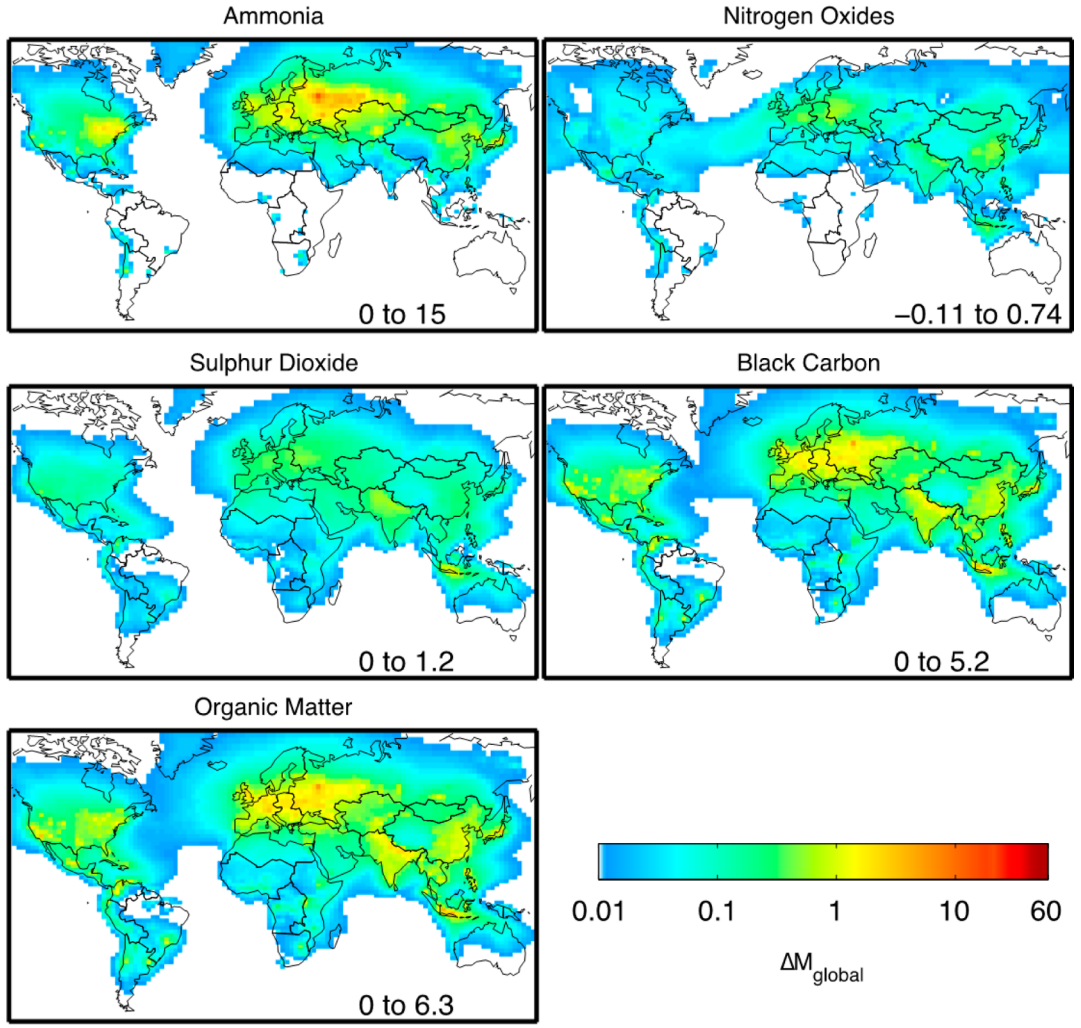

Figure 1. Annual response of global mortality (ΔM_{global}) attributable to a 1 kg km^{-2} yr^{-1} change in local $PM_{2.5}$ precursor emissions. The color in each location indicates how increasing emissions by 1 kg km^{-2} yr^{-1} in that location would change global mortality. Color scale is logarithmic. Numbers in bottom right corner represent range of sensitivities for each map. Solid lines indicate GBD region boundaries. These maps were generated using MATLAB and Mapping Toolbox Release 2013a, The MathWorks, Inc., Natick, Massachusetts, United States.

the dominant, readily modifiable sources that contribute to $PM_{2.5}$ exposure. These groupings also suggest specific control policies, as they tend to come from different human activities. We did not calculate responses to changes in mineral dust, secondary organic aerosol, or sea salt, which are more challenging to modify through policy. Additionally, the current adjoint model does not include secondary organic aerosol. This widely used model is developing rapidly to represent ongoing scientific advances in the challenging area of representing $PM_{2.5}$ concentrations and formation processes. The initial results presented in this proof-of-concept study are expected to evolve with ongoing development.

Global Mortality Attributable to $PM_{2.5}$ Exposure. The ambient concentrations developed in "Estimation of exposure by satellite remote sensing" were applied to a health-impact function to calculate premature mortality for the adjoint cost function described in the previous section, "Adjoint modeling to relate mortality to $PM_{2.5}$ sources." Following Burnett et al.,[33] we calculated the burden of disease due to $PM_{2.5}$ as the number of deaths attributable to four leading causes: ischemic heart disease (IHD), chronic obstructive pulmonary disease (COPD), cerebro-vascular disease (CEV), and lung cancer (LC). Burnett et al.[33] used data from studies including outdoor air pollution, household air pollution and first- and second-hand smoking to provide a concentration−response relationship for concentrations that span the entire range of observed long-term $PM_{2.5}$ concentrations throughout the world. We focused on this concentration−response curve as the most current representation of the disease-specific outcomes for the range of concentrations worldwide.

The relative risk (RR) was calculated as follows:

$$\mathrm{RR} = \begin{cases} 1 + \alpha(1 - e^{-\beta(x-x_0)^{\rho}}), & \text{if } x > x_0 \\ 1, & \text{otherwise} \end{cases} \quad (1)$$

where x is the time-averaged $PM_{2.5}$ concentration at 10 km resolution, x_0 is referred to as the theoretical minimum risk exposure (TMRE), which is defined as the concentration below which it is assumed there are no health effects, and α, β, and ρ are parameters describing the shape of the exposure-response curve. For each cause, we implemented the RR function as in eq 1 using parameters estimated from data from the Monte Carlo simulations performed by Burnett et al.[33] Specific parameters and graphs of the curves are in SI section S-6.

DOI: 10.1021/acs.est.5b00873
Environ. Sci. Technol. 2015, 49, 4335−4344

Table 1. Global Responses to Absolute Changes in Regional Emissions[a]

region	pop(000s)	NH_3	NO_x	SO_2	BC[b]	OM[c]
Asia Pacific, High Income	176 979	13 (1.9)[d]	2.0 (0.23)	3.2 (0.31)	13 (1.7)	16 (2.0)
Asia						
Central	85 845	83 (7.3)	12 (0.61)	21 (1.1)	52 (3.4)	67 (4.3)
East	1 347 974	56 (2.2)	35 (1.6)	28 (1.0)	77 (3.2)	97 (4.0)
South	1 447 648	6.4 (0.41)	16 (0.84)	34 (1.7)	72 (3.7)	91 (4.7)
Southeast	579 605	3.6 (0.38)	8.7 (0.49)	20 (1.3)	62 (4.5)	76 (5.4)
Australasia	24 015	0.015 (0.0011)	0.47 (0.23)	5.1 (0.26)	4.1 (0.23)	5.5 (0.31)
Caribbean	33 239	1.0 (0.32)	1.00 (0.13)	1.8 (0.21)	5.2 (0.67)	6.5 (0.83)
Europe						
Central	132 907	36 (5.3)	10 (1.6)	11 (1.4)	39 (5.7)	49 (7.1)
Eastern	208 488	290 (28)	33 (2.7)	41 (2.6)	160 (13)	200 (17)
Western	400 833	60 (3.9)	13 (7.4)	27 (1.6)	90 (6.2)	110 (7.7)
Latin America						
Andean	51 697	0.64 (0.087)	1.1 (0.14)	1.3 (0.15)	3.7 (0.45)	4.6 (0.55)
Central	219 986	2.5 (0.27)	4.2 (0.38)	8.4 (0.88)	27 (2.9)	33 (3.5)
Southern	59 838	1.9 (0.35)	1.3 (0.29)	2.1 (0.35)	6.6 (1.6)	8.2 (1.9)
Tropical	185 912	0.29 (0.45)	0.49 (0.29)	3.1 (0.74)	5.5 (3.3)	6.9 (4.0)
North Africa/Middle East	395 799	23 (1.0)	10 (0.39)	32 (0.96)	41 (1.6)	54 (2.0)
North America, High Income	326 001	95 (4.7)	18 (0.88)	32 (1.4)	87 (5.2)	110 (6.4)
Oceania	5885	0.087 (0.057)	0.070 (0.065)	0.18 (0.049)	0.50 (0.18)	0.62 (0.21)
Sub-Saharan Africa						
Central	86 332	0.28 (0.043)	0.12 (0.015)	2.0 (0.14)	3.6 (0.31)	4.5 (0.38)
Eastern	306 682	0.52 (0.041)	0.58 (0.039)	6.5 (0.30)	11 (0.85)	13 (1.0)
Southern	65 633	0.66 (0.15)	0.12 (0.024)	1.2 (0.12)	2.1 (0.35)	2.7 (0.43)
Western	281 349	0.97 (0.14)	1.6 (0.12)	5.2 (0.34)	5.3 (0.52)	6.9 (0.65)
total	6 422 647	680 (31)	170 (8.3)	290 (4.8)	760 (19)	960 (24)

[a]Annual global premature mortalities prevented by reducing emissions by 1 kg km^{-2} yr^{-1} in each of 21 GBD regions. [b]BC represents primary black carbon aerosols from fossil fuel, biomass, and biofuel combustion. [c]OM represents primary organic matter aerosols from fossil fuel, biomass, and biofuel combustion. [d]Numbers in brackets represent ±1 error standard deviation.

In order to examine the sensitivity of our results to our choice of health-impact function, we compared the results using the GBD health-impact function against those of two others: (1) curves fit to the GBD RR data with no TMRE,

$$\mathrm{RR} = 1 + \alpha(1 - e^{-\beta x^{\rho}}) \tag{2}$$

and (2) assuming a log−linear response function,

$$\mathrm{RR} = e^{\beta x} \tag{3}$$

with the same parameters as in Anenberg et al.[13]

From these grid-level *RR*s, we calculated country-level population-weighted RRs, using population data from the Gridded Population of the World data set.[36] We then converted these RRs to attributable fractions (AFs) using eq 4:

$$\mathrm{AF} = \frac{\mathrm{RR} - 1}{\mathrm{RR}} = 1 - \frac{1}{\mathrm{RR}} \tag{4}$$

We used country-level demographically weighted, cause-specific mortality data, *M*, from the GBD Project,[37] GPW population, *P*, and the AF to calculate the cost function, *J*, global premature mortality attributable to $PM_{2.5}$ exposure:

$$J = \sum_{k}^{\text{countries}} (P_k \times M_k \times AF_k) \tag{5}$$

We calculated adjoint forcing, the derivative of *J* with respect to model concentrations, at the 2° × 2.5° GEOS-Chem resolution. Following the methods of the GBD project, we assumed that the health effects of exposure to $PM_{2.5}$ are independent of source and composition.[3] $PM_{2.5}$ mass is the most robust indicator of mortality impacts in epidemiologic cohort studies of long-term exposure.[38] This assumption was followed in the GBD, is part of WHO air quality guidelines and the recent International Agency for Research on Cancer's classification of $PM_{2.5}$ as a carcinogen.[39] This assumption also implies the assumption that each of the diseases has the same component-specific sensitivity, which is likely to also be an oversimplification. Exposure is typically a mixture including both primary and secondary PM from a multitude of sources.

SI S-7 presents an evaluation of the adjoint responses. SI section S-8 describes our uncertainty analysis.

RESULTS

Figure 1 shows the modeled marginal damages, that is, the response of global mortality to a 1 kg km^{-2} yr^{-1} change in emissions at 2° × 2.5° resolution. At the level of individual grid cells, the responses ranged from −0.1 premature deaths for NO_x to +15 premature deaths for NH_3. The highest marginal damages were for NH_3 around Moscow (15 deaths kg^{-1} km^2 yr). Primary carbonaceous aerosols had the strongest overall responses of the species we studied, however, marginal damages from NH_3 emissions in eastern Europe and eastern North America exceeded those from organic matter. NH_3 had the strongest response of the secondary inorganic precursors. Responses to absolute changes in organic matter were higher than to black carbon due to differences in hygroscopicity (1 kg of emitted dry OM absorbs more atmospheric water that is retained by $PM_{2.5}$ concentrations at 35% relative humidity).

Marginal damages were generally positive and varied smoothly in space. The overall spatial patterns resembled

DOI: 10.1021/acs.est.5b00873
Environ. Sci. Technol. 2015, 49, 4335−4344

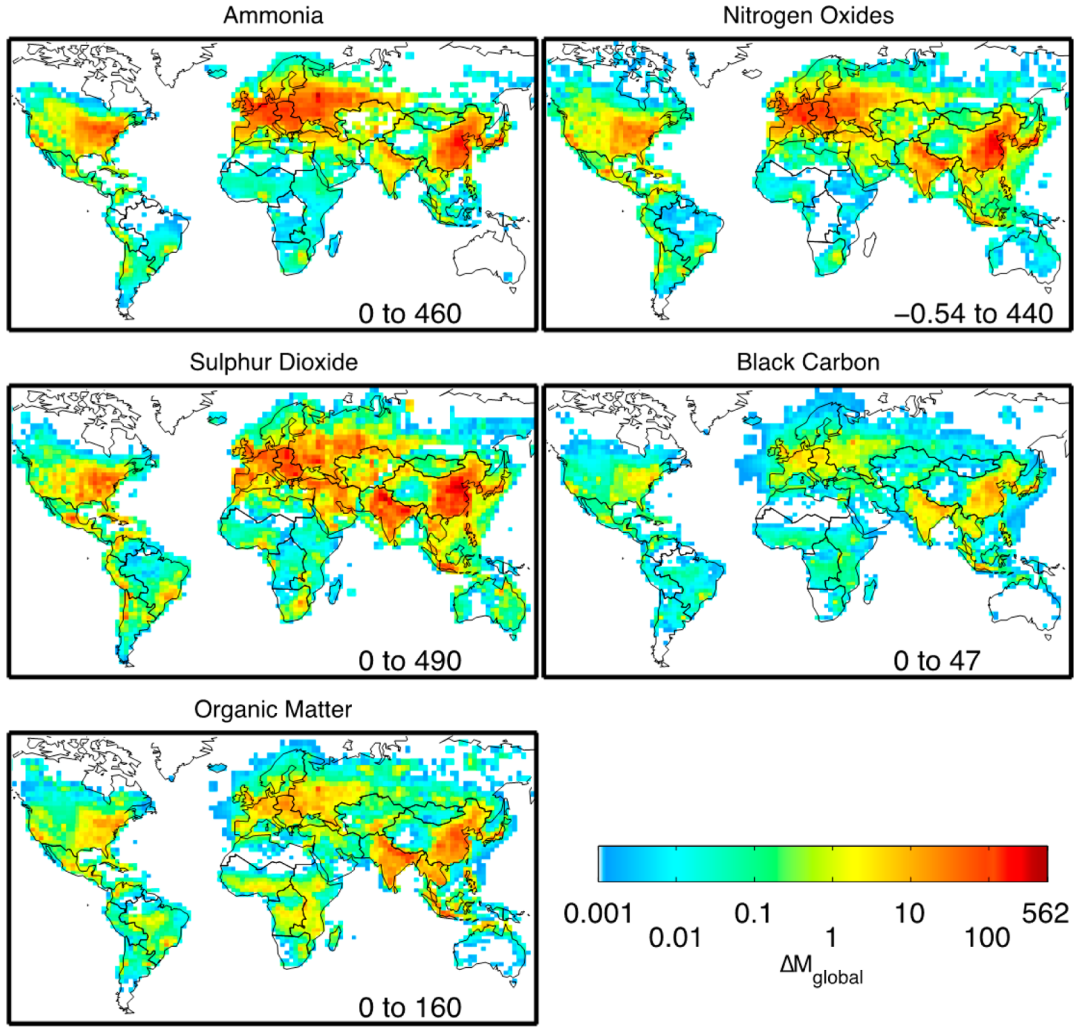

Figure 2. Annual response of global mortality (ΔM_{global}) attributable to a 10% change in local $PM_{2.5}$ precursor emissions. The color in each location indicates how increasing emissions by 10% in that location would change global mortality. Color scale is logarithmic. Numbers in bottom right corner represent range of sensitivities for each map. Solid lines indicate GBD region boundaries. These maps were generated using MATLAB and Mapping Toolbox Release 2013a, The MathWorks, Inc., Natick, Massachusetts, United States.

population density. This was most true for primary carbonaceous aerosols (R = 0.71) and least true for ammonia (R = 0.23), which had a lower response in Northern India than would be expected by following population density. Small positive marginal damages were seen in areas without population, such as over coastal oceans, due to atmospheric transport.

Negative marginal damages, that is, a net reduction in global mortality caused by an increase in emissions, were seen only for NO_x emissions and only in two areas: off the northwestern coast of New Guinea and to the southeast of Iceland, due to nonlinearities in atmospheric chemistry.

Table 1 and SI Figure S3 show marginal damages aggregated by GBD region. The highest modeled regional response to a 1 kg km^{-2} yr^{-1} change was for NH_3 in Eastern Europe (290 attributable deaths kg^{-1} km^2 yr). In all other regions except for Central Asia, primary organic matter had the highest modeled response of the emissions we studied. The marginal damages of BC, OM, and SO_2 emissions in South Asia were within 20% of those of East Asia. However, the modeled response of global mortality to NH_3 emissions in South Asia was an order of magnitude lower than in East Asia (6.4 vs 56 premature deaths per kg NH_3 km^{-2} yr^{-1}).

Figure 2 shows the relative response, or the response in global mortality to a 10% change in emissions at 2° × 2.5° resolution. The responses ranged from −0.5 (NO_x) to 490 (SO_2) global attributable mortalities. Responses to relative changes in emissions of the three inorganic precursors generally exceeded those for primary carbonaceous emissions.

Negative responses were small and again limited to NO_x emissions near New Guinea and Iceland.

Table 2 and SI Figure S4 show modeled responses to a 10% change in emissions aggregated by GBD region. The highest response was for SO_2 in East Asia (10 000 deaths). No single emission type dominated. East Asian emissions produced the highest response for all 5 emission types. Responses were noteworthy for Western Europe for NO_x (3900 deaths) and South Asia for SO_2 emissions (5600 deaths).

SI Table S-4 shows the rankings of the top 5 regions. Eastern Europe ranked first or second in marginal damages for all species we studied. East Asia ranked highest in all relative sensitivities.

DOI: 10.1021/acs.est.5b00873
Environ. Sci. Technol. 2015, 49, 4335−4344

Table 2. Global Responses to Relative Changes in Regional Emissions[a]

region	pop(000s)	NH_3	NO_x	SO_2	BC[b]	OM[c]
Asia Pacific, High Income	176 979	730 (150)[d]	730 (140)	500 (69)	120 (26)	240 (51)
Asia						
Central	85 845	400 (57)	180 (24)	860 (97)	16 (1.7)	160 (18)
East	1 347 974	5800 (440)	8000 (670)	10000 (730)	550 (41)	2300 (170)
South	1 447 648	500 (42)	1600 (130)	5600 (460)	330 (25)	2000 (160)
Southeast	579 605	89 (8.4)	430 (36)	1100 (120)	170 (19)	1100 (110)
Australasia	24 015	0.066 (0.010)	2.1 (0.24)	74 (11)	3.3 (0.49)	57 (8.7)
Caribbean	33 239	8.2 (1.9)	34 (5.1)	99 (15)	2.5 (0.34)	15 (2.1)
Europe						
Central	132 907	2400 (380)	2100 (340)	2800 (420)	72 (13)	350 (61)
Eastern	208 488	5400 (740)	2600 (370)	3200 (420)	100 (25)	670 (140)
Western	400 833	4000 (360)	3900 (460)	2200 (200)	150 (16)	360 (38)
Latin America						
Andean	51 697	9.4 (1.5)	18 (2.3)	110 (27)	2.0 (0.39)	17 (3.8)
Central	219 986	84 (17)	290 (61)	470 (90)	25 (4.2)	140 (22)
Southern	59 838	29 (6.6)	37 (11)	200 (49)	6.8 (5.3)	28 (17)
Tropical	185 912	14 (26)	38 (52)	140 (100)	11 (15)	85 (70)
North Africa/Middle East	395 799	310 (22)	270 (16)	1900 (100)	18 (1.4)	74 (4.8)
North America, High Income	326 001	2600 (170)	1800 (120)	2100 (140)	150 (16)	620 (49)
Oceania	5885	0.50 (0.62)	0.063 (0.14)	0.14 (0.062)	0.018 (0.0062)	0.14 (0.047)
Sub-Saharan Africa						
Central	86 332	0.96 (0.18)	0.70 (0.16)	22 (5.3)	5.6 (0.58)	90 (8.3)
Eastern	306 682	6.1 (0.59)	1.5 (0.19)	40 (6.8)	13 (1.6)	160 (16)
Southern	65 633	13 (3.7)	10 (6.2)	96 (27)	2.4 (0.75)	19 (5.0)
Western	281 349	12 (5.9)	8.1 (2.8)	48 (19)	5.1 (1.0)	70 (13)
total	6 422 647	22000 (1000)	22000 (990)	32000 (1100)	1800 (71)	8500 (320)

[a]Annual global premature mortalities prevented by reducing emissions by 10% in each of 21 GBD regions. [b]BC represents primary black carbon aerosols from fossil fuel, biomass, and biofuel combustion. [c]OM represents primary organic matter aerosols from fossil fuel, biomass, and biofuel combustion. [d]Numbers in brackets represent ±1 error standard deviation.

For the health-impact function without a TMRE (eq 2), the spatial pattern of the responses was nearly identical ($R = 0.98$) to those presented here, with differences in magnitude of up to 20%.

The results obtained using a log−linear health-impact function also were spatially similar ($R = 0.85$) to the results using the base GBD health-impact function, however responses in South and East Asia were roughly 60% stronger.

DISCUSSION

This study examined the response of global $PM_{2.5}$-related mortality to changes in precursor emissions. The responses presented here are based on current scientific understanding of the factors affecting global $PM_{2.5}$ concentrations, combined with current scientific understanding of $PM_{2.5}$-related mortality. The exposure distribution, exposure-response functions, and mortality distribution used in this study build from the substantial effort undertaken as part of the GBD project. The responses generated using this novel method can therefore highlight some important geographical patterns, such as the large global benefits from reducing South Asian SO_2 emissions instead of NH_3 emissions. We presented responses to both absolute and relative changes in emissions. Responses to absolute changes (i.e., marginal damages) are more easily interpreted since they are less dependent on the initial emission rates. Responses to relative changes are of more relevance for some policy applications such as reducing vehicle-miles traveled.

In general, the response of global mortality to changes in precursor emissions was proportional to population distribution. Responses were enhanced by high relevant baseline mortality rates in Eastern Europe, East Asia, and Indonesia. The relationship of population with relative responses was stronger than with marginal damages because emissions tend to be correlated with population. Precursor emissions near dense populations have the largest opportunity to affect exposure. Long-range transport also can be important and has been extensively studied.[40] Some indication of the distances over which transport affects exposure can be seen in Figure 1, where responses >0.01 death kg^{-1} km^2 yr can be seen over the ocean hundreds of kilometers from populated shorelines.

Striking regional differences were found in responses. Global mortality was 2−10 times less sensitive to relative changes in emissions from South Asia than from East Asia, in part because emissions and relevant baseline mortality rates in the South Asia region tend to be lower. Eastern Europe ranked first in marginal damages to all emissions studied except SO_2, in part due to high regional relevant baseline mortality rates for the diseases related to air pollution. Furthermore, the baseline $PM_{2.5}$ concentrations in Eastern Europe make the *RR* highly sensitive (4−10 times more sensitive than Eastern China or Northern India) to changes in $PM_{2.5}$ concentrations because the slope of the *RR* curve decreases with increasing $PM_{2.5}$ concentrations (SI Figure S-2).

Primary carbonaceous aerosols had the strongest overall marginal damages because carbonaceous material is emitted as particulate matter, whereas with secondary inorganics, only in limiting cases will precursor gases undergo 100% conversion to the aerosol phase. Fann et al.[41] similarly found large marginal

DOI: 10.1021/acs.est.5b00873
Environ. Sci. Technol. 2015, 49, 4335−4344

damages from carbonaceous emissions compared with emissions from secondary inorganic precursors.

NH_3 marginal impact was both the strongest response of the secondary inorganic precursors and the least related to population. Formation of $PM_{2.5}$ as $(NH_4)_2SO_4$, NH_4HSO_4, or NH_4NO_3 yields more mass formed than emitted. Low responses in northern India arise from a large reservoir of NH_3 that has already reacted with the available SO_4^{2-} and NO_3^-. Our results are consistent with a recent European Topic Centre review that found overall, NH_3 was likely to be the most important $PM_{2.5}$ precursor species for continental Europe and especially the United Kingdom.[42] Nonetheless, our NH_3 responses may be greater than actual responses in maritime-influenced regions such as the Mediterranean, because the Na^+-NO_3^- reaction[43] is not included in the aerosol thermodynamics in the model version we used. Our NH_3 sensitivities in Europe were 0.4 to 0.8 of the original values for the month of January when we decreased NO_x emissions by 50% to simulate losing NO_3^- to $NaNO_3$.

Our finite difference tests (SI section S-7) indicated that conclusions drawn from these responses were as good as those calculated by perturbing emissions to the forward model for a range of changes in emissions up to at least 10% from current rates. Moreover, these local sensitivities for several species were calculated using approximately three times the computing resources of a single forward model run. Computing local sensitivities by the finite-difference method of perturbing emissions would require tens of thousands of forward model runs.

The dominant sources of uncertainty in the simulation responses arose from representation of $PM_{2.5}$-formation processes and from uncertainty in health-impact function parameters (SI section S-8). The quality of the results from this method will continue to improve as results from region-specific $PM_{2.5}$ mortality cohort studies become available, and as higher-resolution simulations better capture the relation between $PM_{2.5}$ and emissions.[44]

It is possible that the model has missed not only the magnitude, but also the sign of the true sensitivity, as a result of nonlinearities in the $PM_{2.5}$ formation process and differences between the true state of the atmosphere and the modeled state caused, for example, by processes not included in the model. In the future, the very tool we used in this study, the adjoint, could be used to assimilate observations, improving the accuracy of emission inventories and model parameters so that the modeled state better represents the true state.[21]

The exposure response function produced by Burnett et al.[33] included a TMRE. In order to represent this, our fit parameters included a TMRE ranging from 7.0 for IHD to 8.4 for stroke. Epidemiological research to date has not found an exposure threshold where $PM_{2.5}$ reductions provided no benefit.[45,46] For example, a recent population-based study in Canada observed no deviation from linearity in the relationship between concentrations and mortality even at concentrations as low as 5 $\mu g/m^3$, which is approaching the lowest measured concentrations in populated areas.[46] Eliminating the TMRE linearly changed our results (R = 0.98), indicating that the spatial relationships we found are robust.

Like the GBD project, this study assumed that the health effects of exposure to $PM_{2.5}$ are independent of source or composition. While this may not be true, the current evidence is insufficient to determine composition-dependent exposure-response curves. The role of chemical composition as a determinant of toxicity attributable to ambient particulate matter is an active research area.[47,48] Future changes to exposure-response functions, which incorporate information about $PM_{2.5}$ composition, could be readily incorporated into the framework presented here, for example by applying component-specific concentration−response functions. Other metrics such as disability-adjusted life years or monetary health benefits could also readily be implemented.

We calculated these sensitivities based on population distributions, demographics, and relevant baseline mortality rates from the year 2005, and for that reason our estimates pertain to the burden of disease attributable to exposure to $PM_{2.5}$ in 2005 and should not be assumed to reflect the burden that might be avoided in the future.[49] Changes to the burden of disease due to exposure to $PM_{2.5}$ that might be expected to occur in the future as a result of changes in the relative contribution of various pollution sources would depend importantly on future cause-specific mortality rates for cardiovascular and respiratory diseases, and lung cancer. These rates changed dramatically between 1990 and 2010 and would be expected to change further in the future due to changes in population age distributions and other factors.[37,50] Increasing urbanization is also likely to change exposure to particulate matter.[51] Therefore, it is advisible to periodically update this analysis to reflect current demographics and exposure in future.

In this study, changes in global mortality were not attributed to a particular area. These results are, therefore, most relevant to global policy. In order to determine how mortality in a specific area is affected by changes in another (or the same) specific area, the adjoint would need to be run with the cost function defined for the area of interest. This is planned for future study of country-specific mortality.

In summary, we used the adjoint of the GEOS-Chem chemical transport model to efficiently determine the response of global mortality to changes in local emissions. We found that global mortality exhibited dramatic differences in sensitivity to emissions from different regions or different emission types. Overall, global mortality was more sensitive to absolute changes in emissions of primary carbonaceous aerosols than of secondary inorganic precursors. The highest responses for relative changes were found in secondary inorganic precursor emissions from China and in SO_2 emissions from India. These responses imply regionally dependent policies, even when the regions have similar populations. For example, controls on agricultural emissions of NH_3 in East Asia could prevent 10 times more premature deaths than would these same controls in South Asia. Our results also suggest that the benefits of China's recent controls on SO_2 emissions may be partially offset by rising NO_x and NH_3 emissions.

■ ASSOCIATED CONTENT

Supporting Information

Impacts of resolution; full description of the GEOS-Chem model and its adjoint; evaluation of speciated model concentrations; model emissions used; full description of the cost function; integrated exposure response parameters; evaluation of adjoint responses; description of uncertainty analysis; tables of responses by GBD region; and ranking of top-contributing regions to global mortality. This material is available free of charge via the Internet at http://pubs.acs.org.

DOI: 10.1021/acs.est.5b00873
Environ. Sci. Technol. 2015, 49, 4335−4344

AUTHOR INFORMATION

Corresponding Author

*Phone: (902) 494-1820; fax: (902) 494-5191; e-mail: colin.lee@dal.ca.

Notes

The authors declare no competing financial interest.

ACKNOWLEDGMENTS

This work was supported by Natural Sciences and Engineering Research Council of Canada. D.H. was supported by NASA AQAST NNX11AI54G. We thank Richard T. Burnett from Health Canada for providing the relative risk data. We also thank Christopher J L Murray, Stephen Lim, Rafael Lozano, and Haidon Wang from the Institute for Health Metrics and Evaluation, University of Washington for providing mortality rates.

ABBREVIATIONS

AOD	aerosol optical depth
AF	attributable fraction
BC	black carbon
CEV	cerebrovascular disease
COPD	chronic obstructive pulmonary disease
GBD	Global Burden of Disease
IHD	ischemic heart disease
LC	lung cancer
OC	organic carbon
OM	organic matter
$PM_{2.5}$	particulate matter with a diameter ≤ 2.5 μm
RR	relative risk
TMRE	theoretical minimum risk exposure

REFERENCES

(1) Dockery, D. W.; Pope, I. C. A.; Xu, X.; Spengler, J. D.; Ware, J. H.; Faye, M. E.; Ferris, B. G. J.; Speizer, F. E. An association between air pollution and mortality in six U.S. cities. *N. Engl. J. Med.* **1993**, *329*, 1753−1759.

(2) Jerrett, M.; Burnett, R.; Ma, R.; Pope, C.; Krewski, D.; Newbold, K.; Thurston, G.; Shi, Y.; Finkelstein, N.; Calle, E.; Thun, M. Spatial analysis of air pollution and mortality in Los Angeles. *Epidemiology* **2005**, *16*, 727−736.

(3) Lim, S. S.; Vos, T.; Flaxman, A. D.; Danaei, G.; Shibuya, K.; Adair-Rohani, H.; Amann, M.; Anderson, H. R.; Andrews, K. G.; Aryee, M.; Atkinson, C.; Bacchus, L. J.; Bahalim, A. N.; Balakrishnan, K.; Balmes, J.; Barker-Collo, S.; Baxter, A.; Bell, M. L.; Blore, J. D.; Blyth, F.; Bonner, C.; Borges, G.; Bourne, R.; Boussinesq, M.; Brauer, M.; Brooks, P.; Bruce, N. G.; Brunekreef, B.; Bryan-Hancock, C.; Bucello, C.; Buchbinder, R.; Bull, F.; Burnett, R. T.; Byers, T. E.; Calabria, B.; Carapetis, J.; Carnahan, E.; Chafe, Z.; Charlson, F.; Chen, H.; Chen, J. S.; Cheng, A. T.; Child, J. C.; Cohen, A.; Colson, K. E.; Cowie, B. C.; Darby, S.; Darling, S.; Davis, A.; Degenhardt, L.; Dentener, F.; Des Jarlais, D. C.; Devries, K.; Dherani, M.; Ding, E. L.; Dorsey, E. R.; Driscoll, T.; Edmond, K.; Ali, S. E.; Engell, R. E.; Erwin, P. J.; Fahimi, S.; Falder, G.; Farzadfar, F.; Ferrari, A.; Finucane, M. M.; Flaxman, S.; Fowkes, F. G. R.; Freedman, G.; Freeman, M. K.; Gakidou, E.; Ghosh, S.; Giovannucci, E.; Gmel, G.; Graham, K.; Grainger, R.; Grant, B.; Gunnell, D.; Gutierrez, H. R.; Hall, W.; Hoek, H. W.; Hogan, A.; Hosgood, H. D.; Hoy, D.; Hu, H.; Hubbell, B. J.; Hutchings, S. J.; Ibeanusi, S. E.; Jacklyn, G. L.; Jasrasaria, R.; Jonas, J. B.; Kan, H.; Kanis, J. A.; Kassebaum, N.; Kawakami, N.; Khang, Y.; Khatibzadeh, S.; Khoo, J.; Kok, C.; Laden, F.; Lalloo, R.; Lan, Q.; Lathlean, T.; Leasher, J. L.; Leigh, J.; Li, Y.; Lin, J. K.; Lipshultz, S. E.; London, S.; Lozano, R.; Lu, Y.; Mak, J.; Malekzadeh, R.; Mallinger, L.; Marcenes, W.; March, L.; Marks, R.; Martin, R.; McGale, P.; McGrath, J.; Mehta, S.; Mensah, G. A.; Merriman, T. R.; Micha, R.; Michaud, C.; Mishra, V.; Hanafiah, K. M.; Mokdad, A. A.; Morawska, L.; Mozaffarian, D.; Murphy, T.; Naghavi, M.; Neal, B.; Nelson, P. K.; Nolla, J. M.; Norman, R.; Olives, C.; Omer, S. B.; Orchard, J.; Osborne, R.; Ostro, B.; Page, A.; Pandey, K. D.; Parry, C. D.; Passmore, E.; Patra, J.; Pearce, N.; Pelizzari, P. M.; Petzold, M.; Phillips, M. R.; Pope, D.; Pope, C. A.; Powles, J.; Rao, M.; Razavi, H.; Rehfuess, E. A.; Rehm, J. T.; Ritz, B.; Rivara, F. P.; Roberts, T.; Robinson, C.; Rodriguez-Portales, J. A.; Romieu, I.; Room, R.; Rosenfeld, L. C.; Roy, A.; Rushton, L.; Salomon, J. A.; Sampson, U.; Sanchez-Riera, L.; Sanman, E.; Sapkota, A.; Seedat, S.; Shi, P.; Shield, K.; Shivakoti, R.; Singh, G. M.; Sleet, D. A.; Smith, E.; Smith, K. R.; Stapelberg, N. J.; Steenland, K.; StË†ckl, H.; Stovner, L. J.; Straif, K.; Straney, L.; Thurston, G. D.; Tran, J. H.; Van Dingenen, R.; van Donkelaar, A.; Veerman, J. L.; Vijayakumar, L.; Weintraub, R.; Weissman, M. M.; White, R. A.; Whiteford, H.; Wiersma, S. T.; Wilkinson, J. D.; Williams, H. C.; Williams, W.; Wilson, N.; Woolf, A. D.; Yip, P.; Zielinski, J. M.; Lopez, A. D.; Murray, C. J.; Ezzati, M. A comparative risk assessment of burden of disease and injury attributable to 67 risk factors and risk factor clusters in 21 regions, 1990 & 2010: a systematic analysis for the Global Burden of Disease Study 2010. *Lancet* **2012**, *380*, 2224−2260.

(4) United States Environmental Protection Agency. *The Benefits and Costs of the Clean Air Act 1990 to 2010*. 1999.

(5) Krupnick, A.; Morgenstern, R. The future of benefit-cost analyses of the Clean Air Act. *Annu. Rev. Public Health* **2002**, *23*, 427−448.

(6) Cox, L. A. T. Reassessing the Human Health Benefits from Cleaner Air. *Risk Anal.* **2012**, *32*, 816−829.

(7) Bell, M. L.; Morgenstern, R. D.; Harrington, W. Quantifying the human health benefits of air pollution policies: Review of recent studies and new directions in accountability research. *Environ. Sci. Policy* **2011**, *14*, 357−368.

(8) Li, Y.; Wang, W.; Kan, H.; Xu, X.; Chen, B. Air quality and outpatient visits for asthma in adults during the 2008 Summer Olympic Games in Beijing. *Sci. Total Environ.* **2010**, *408*, 1226−1227.

(9) Hou, Q.; An, X. Q.; Wang, Y.; Guo, J. P. An evaluation of resident exposure to respirable particulate matter and health economic loss in Beijing during Beijing 2008 Olympic Games. *Sci. Total Environ.* **2010**, *408*, 4026−4032.

(10) Wu, S.; Deng, F.; Niu, J.; Huang, Q.; Liu, Y.; Gu, X. Association of Heart Rate Variability in Taxi Drivers with Marked Changes in Particulate Air Pollution in Beijing in 2008. *Environ. Health Perspect.* **2010**, *118*, 87−91.

(11) United States Environmental Protection Agency. *Benefits and Costs of the Clean Air Act: 1970 to 1990*, 1997.

(12) Chay, K.; Dobkin, C.; Greenstone, M. The Clean Air Act of 1970 and adult mortality. *J. Risk Uncertainty* **2003**, *27*, 279−300.

(13) Anenberg, S. C.; Horowitz, L. W.; Tong, D. Q.; West, J. J. An estimate of the global burden of anthropogenic ozone and fine particulate matter on premature human mortality using atmospheric modeling. *Environ. Health Perspect.* **2010**, *118*, 1189−1195.

(14) West, J. J.; Naik, V.; Horowitz, L. W.; Fiore, A. M. Effect of regional precursor emission controls on long-range ozone transport—Part 1: Short-term changes in ozone air quality. *Atmos. Chem. Phys.* **2009**, *9*, 6077−6093.

(15) Anenberg, S. C.; West, J. J.; Fiore, A. M.; Jaffe, D. A.; Prather, M. J.; Bergmann, D.; Cuvelier, K.; Dentener, F. J.; Duncan, B. N.; Gauss, M.; Hess, P.; Jonson, J. E.; Lupu, A.; MacKenzie, I. A.; Marmer, E.; Park, R. J.; Sanderson, M. G.; Schultz, M.; Shindell, D. T.; Szopa, S.; Garcia Vivanco, M.; Wild, O.; Zang, G. Intercontinental impacts of ozone pollution on human mortality. *Environ. Sci. Technol.* **2009**, *43*, 6482−6487.

(16) Liu, J.; Mauzerall, D. L.; Horowitz, L. W. Evaluating inter-continental transport of fine aerosols: (2) Global health impact. *Atmos. Environ.* **2009**, *43*, 4339−4347.

(17) Saikawa, E.; Kurokawa, J.; Takigawa, M.; Borken-Kleefeld, J.; Mauzerall, D. L.; Horowitz, L. W.; Ohara, T. The impact of China's vehicle emissions on regional air quality in 2000 and 2020: A scenario analysis. *Atmos. Chem. Phys.* **2011**, *11*, 9465−9484.

DOI: 10.1021/acs.est.5b00873
Environ. Sci. Technol. 2015, 49, 4335−4344

(18) Henze, D. K.; Hakami, A.; Seinfeld, J. H. Development of the adjoint of GEOS-Chem. *Atmos. Chem. Phys.* **2007**, *7*, 2413−2433.
(19) Henze, D. K.; Seinfeld, J. H.; Shindell, D. T. Inverse modeling and mapping U.S. air quality influences of inorganic PM2.5 precursor emissions using the adjoint of GEOS-Chem. *Atmos. Chem. Phys.* **2009**, *9*, 5877−5903.
(20) Wang, J.; Xu, X.; Henze, D. K.; Zeng, J.; Ji, Q.; Tsay, S.; Huang, J. Top-down estimate of dust emissions through integration of MODIS and MISR aerosol retrievals with the GEOS-Chem adjoint model. *Geophys. Res. Lett.* **2012**, *39*.
(21) Xu, X.; Wang, J.; Henze, D. K.; Qu, W.; Kopacz, M. Constraints on aerosol sources using GEOS-Chem adjoint and MODIS radiances, and evaluation with multisensor (OMI MISR) data. *J. Geophys. Res.: Atmos.* **2013**, *118*, 6396−6413.
(22) Koo, J.; Wang, Q.; Henze, D. K.; Waitz, I. A.; Barrett, S. R. H. Spatial sensitivities of human health risk to intercontinental and high-altitude pollution. *Atmos. Environ.* **2013**, *71*, 140−147.
(23) Pappin, A. J.; Hakami, A. Source attribution of health benefits from air pollution abatement in Canada and the United States: An adjoint sensitivity analysis. *Environ. Health Perspect.* **2013**, *121*, 572−579.
(24) Klimont, Z.; Smith, S. J.; Cofala, J. The last decade of global anthropogenic sulfur dioxide: 2000−2011 emissions. *Environ. Res. Lett.* **2013**, *8*, 014003.
(25) Boys, B. L.; Martin, R. V.; van Donkelaar, A.; MacDonell, R.; Hsu, N. C.; Cooper, M. J.; Yantosca, R. M.; Lu, Z.; Streets, D. G.; Zhang, Q.; Wang, S. Fifteen-year global time series of satellite-derived fine particulate matter. *Environ. Sci. Technol.* **2014**, *48*, 11109−11118.
(26) van Donkelaar, A.; Martin, R. V.; Brauer, M.; Boys, B. L. Use of satellite observations for long-term exposure assessment of global concentrations of fine particulate matter. *Environ. Health Perspect.* **2015**, *123*, 135−143.
(27) Galloway, J. N.; Townsend, A. R.; Erisman, J. W.; Bekunda, M.; Cai, Z.; Freney, J. R.; Martinelli, L. A.; Seitzinger, S. P.; Sutton, M. A. Transformation of the nitrogen cycle: Recent trends, questions, and potential solutions. *Science* **2008**, *320*, 889−892.
(28) Wang, S.; Xing, J.; Jang, C.; Zhu, Y.; Fu, J. S.; Hao, J. Impact assessment of ammonia emissions on inorganic aerosols in East China using response surface modeling technique. *Environ. Sci. Technol.* **2011**, *45*, 9293−9300.
(29) Kurokawa, J.; Ohara, T.; Morikawa, T.; Hanayama, S.; Janssens-Maenhout, G.; Fukui, T.; Kawashima, K.; Akimoto, H. Emissions of air pollutants and greenhouse gases over Asian regions during 2000−2008: Regional emission inventory in Asia (REAS) version 2. *Atmos. Chem. Phys.* **2013**, *13*, 11019−11058.
(30) Bey, I.; Jacob, D.; Yantosca, R.; Logan, J.; Field, B.; Fiore, A.; Li, Q.; Liu, H.; Mickley, L.; Schultz, M. Global modeling of tropospheric chemistry with assimilated meteorology: Model description and evaluation. *J. Geophys. Res.: Atmos.* **2001**, *106*, 23073−23095.
(31) Park, R. J.; Jacob, D. J.; Field, B. D.; Yantosca, R. M.; Chin, M. Natural and transboundary pollution influences on sulfate-nitrate-ammonium aerosols in the United States: Implications for policy. *J. Geophys. Res.: Atmos.* **2004**, *109*, D15204.
(32) van Donkelaar, A.; Martin, R. V.; Brauer, M.; Kahn, R.; Levy, R.; Verduzco, C.; Villeneuve, P. J. Global estimates of ambient fine particulate matter concentrations from satellite-based aerosol optical depth: Development and application. *Environ. Health Perspect.* **2010**, *118*, 847−855.
(33) Burnett, R. T.; Pope, C. A. I.; Ezzati, M.; Olives, C.; Lim, S. S.; Mehta, S.; Shin, H. H.; Singh, G.; Hubbell, B.; Brauer, M.; Anderson, H. R.; Smith, K. R.; Kan, H.; Laden, F.; Pruess, A.; Turner, M. C.; Thun, M.; Cohen, A. An integrated risk function for estimating the global burden of disease attributable to ambient fine particulate matter exposure. *Environ. Health Perspect.* **2014**, *122*, 397−403.
(34) Punger, E. M.; West, J. J. The effect of grid resolution on estimates of the burden of ozone and fine particulate matter on premature mortality in the U.S.A. *Air Qual., Atmos. Health* **2013**, 1−11.
(35) Brauer, M.; Amann, M.; Burnett, R. T.; Cohen, A.; Dentener, F.; Ezzati, M.; Henderson, S. B.; Krzyzanowski, M.; Martin, R. V.; Van Dingenen, R.; van Donkelaar, A.; Thurston, G. D. Exposure assessment for estimation of the global burden of disease attributable to outdoor air pollution. *Environ. Sci. Technol.* **2012**, *46*, 652−660.
(36) Center for International Earth Science Information Network (CIESIN); Centro Internacional de Agricultura Tropical (CIAT) Gridded Population of the World, Version 3 (GPWv3): Population Count Grid, Future Estimates. **2005**.
(37) Lozano, R.; Naghavi, M.; Foreman, K.; Lim, S.; Shibuya, K.; Aboyans, V.; Abraham, J.; Adair, T.; Aggarwal, R.; Ahn, S. Y.; Alvarado, M.; Anderson, H. R.; Anderson, L. M.; Andrews, K. G.; Atkinson, C.; Baddour, L. M.; Barker-Collo, S.; Bartels, D. H.; Bell, M. L.; Benjamin, E. J.; Bennett, D.; Bhalla, K.; Bikbov, B.; Bin Abdulhak, A.; Birbeck, G.; Blyth, F.; Bolliger, I.; Boufous, S. A.; Bucello, C.; Burch, M.; Burney, P.; Carapetis, J.; Chen, H.; Chou, D.; Chugh, S. S.; Coffeng, L. E.; Colan, S. D.; Colquhoun, S.; Colson, K. E.; Condon, J.; Connor, M. D.; Cooper, L. T.; Corriere, M.; Cortinovis, M.; de Vaccaro, K. C.; Couser, W.; Cowie, B. C.; Criqui, M. H.; Cross, M.; Dabhadkar, K. C.; Dahodwala, N.; De Leo, D.; Degenhardt, L.; Delossantos, A.; Denenberg, J.; Des Jarlais, D. C.; Dharmaratne, S. D.; Dorsey, E. R.; Driscoll, T.; Duber, H.; Ebel, B.; Erwin, P. J.; Espindola, P.; Ezzati, M.; Feigin, V.; Flaxman, A. D.; Forouzanfar, M. H.; Fowkes, F. G. R.; Franklin, R.; Fransen, M.; Freeman, M. K.; Gabriel, S. E.; Gakidou, E.; Gaspari, F.; Gillum, R. F.; Gonzalez-Medina, D.; Halasa, Y. A.; Haring, D.; Harrison, J. E.; Havmoeller, R.; Hay, R. J.; Hoen, B.; Hotez, P. J.; Hoy, D.; Jacobsen, K. H.; James, S. L.; Jasrasaria, R.; Jayaraman, S.; Johns, N.; Karthikeyan, G.; Kassebaum, N.; Keren, A.; Khoo, J.; Knowlton, L. M.; Kobusingye, O.; Koranteng, A.; Krishnamurthi, R.; Lipnick, M.; Lipshultz, S. E.; Ohno, S. L.; Mabweijano, J.; MacIntyre, M. F.; Mallinger, L.; March, L.; Marks, G. B.; Marks, R.; Matsumori, A.; Matzopoulos, R.; Mayosi, B. M.; McAnulty, J. H.; McDermott, M. M.; McGrath, J.; Mensah, G. A.; Merriman, T. R.; Michaud, C.; Miller, M.; Miller, T. R.; Mock, C.; Mocumbi, A. O.; Mokdad, A. A.; Moran, A.; Mulholland, K.; Nair, M. N.; Naldi, L.; Narayan, K. M. V.; Nasseri, K.; Norman, P.; O'Donnell, M.; Omer, S. B.; Ortblad, K.; Osborne, R.; Ozgediz, D.; Pahari, B.; Pandian, J. D.; Rivero, A. P.; Padilla, R. P.; Perez-Ruiz, F.; Perico, N.; Phillips, D.; Pierce, K.; Pope, I. C.; Arden; Porrini, E.; Pourmalek, F.; Raju, M.; Ranganathan, D.; Rehm, J. T.; Rein, D. B.; Remuzzi, G.; Rivara, F. P.; Roberts, T.; De Leon, F. R.; Rosenfeld, L. C.; Rushton, L.; Sacco, R. L.; Salomon, J. A.; Sampson, U.; Sanman, E.; Schwebel, D. C.; Segui-Gomez, M.; Shepard, D. S.; Singh, D.; Singleton, J.; Sliwa, K.; Smith, E.; Steer, A.; Taylor, J. A.; Thomas, B.; Tleyjeh, I. M.; Towbin, J. A.; Truelsen, T.; Undurraga, E. A.; Venketasubramanian, N.; Vijayakumar, L.; Vos, T.; Wagner, G. R.; Wang, M.; Wang, W.; Watt, K.; Weinstock, M. A.; Weintraub, R.; Wilkinson, J. D.; Woolf, A. D.; Wulf, S.; Yeh, P.; Yip, P.; Zabetian, A.; Zheng, Z.; Lopez, A. D.; Murray, C. J. L. Global and regional mortality from 235 causes of death for 20 age groups in 1990 and 2010: A systematic analysis for the Global Burden of Disease Study 2010. *Lancet* **2012**, *380*, 2095−2128.
(38) Chen, H.; Goldberg, M. S.; Villeneuve, P. J. A systematic review of the relation between long-term exposure to ambient air pollution and chronic diseases. *Rev. Environ. Health* **2008**, *23*, 243−297.
(39) Loomis, D.; Grosse, Y.; Lauby-Secretan, B.; Ghissassi, F. E.; Bouvard, V.; Benbrahim-Tallaa, L.; Guha, N.; Baan, R.; Mattock, H.; Straif, K. The carcinogenicity of outdoor air pollution. *Lancet Oncol.* **2013**, *14*, 1262−1263.
(40) Task Force on Hemispheric Transport of Air Pollution Hemispheric transport of air pollution 2010: Part A: Ozone and Particulate Matter . 2010, *17*.
(41) Fann, N.; Fulcher, C.; Hubbell, B. The influence of location, source, and emission type in estimates of the human health benefits of reducing a ton of air pollution. *Air Qual., Atmos. Health* **2009**, *2*, 169−176.
(42) Beauchamp, M.; Bessagnet, B.; Guerreiro, C.; de Leeuw, F.; Tsyro, S.; Ruyssenaars, P.; Sauter, F.; Velders, G.; Meleux, F.; Colette, A.; Rouïl, L. *Sensitivity Analysis of Ammonia Emission Reductions on Exceedances of PM Air Quality Standards*; Technical Report for European Topic Centre on Air Pollution and Climate Change Mitigation, 2013

DOI: 10.1021/acs.est.5b00873
Environ. Sci. Technol. 2015, 49, 4335−4344

(43) Athanasopoulou, E.; Tombrou, M.; Pandis, S. N.; Russell, A. G. The role of sea-salt emissions and heterogeneous chemistry in the air quality of polluted coastal areas. *Atmos. Chem. Phys.*, *5755*.
(44) Cohan, D. S.; Napelenok, S. L. Air quality response modeling for decision support. *Atmosphere* **2011**, *2*, 407−425.
(45) Correia, A. W.; Pope, I. C.A.; Dockery, D. W.; Wang, Y.; Ezzati, M.; Dominici, F. Effect of air pollution control on life expectancy in the United States: An analysis of 545 U.S. counties for the period from 2000 to 2007. *Epidemiology* **2013**, *24*, 23−31.
(46) Crouse, D. L.; Peters, P. A.; van Donkelaar, A.; Goldberg, M. S.; Villeneuve, P. J.; Brion, O.; Khan, S.; Atari, D. O.; Jerrett, M.; Pope, I. C. A.; Brauer, M.; Brook, J. R.; Martin, R. V.; Stieb, D.; Burnett, R. T. Risk of non accidental and cardiovascular mortality in relation to long-term exposure to low concentrations of fine particulate matter: A Canadian national-level cohort study. *Environ. Health Perspect.* **2012**, *120*, 708−714.
(47) Heal, M. R.; Kumar, P.; Harrison, R. M. Particles, air quality, policy and health. *Chem. Soc. Rev.* **2012**, *41*, 6606−6630.
(48) Kelly, F. J.; Fussell, J. C. Size, source and chemical composition as determinants of toxicity attributable to ambient particulate matter. *Atmos. Environ.* **2012**, *60*, 504−526.
(49) Murray, C. J.; Ezzati, M.; Lopez, A.; Rodgers, A.; Vander Hoorn, S. In *Comparative Quantification of Health Risk: Conceptual Framework and Methodological Issues*; Ezzati, M., Lopez, A. D., Rodgers, A., Murray, C. J., Eds.; Comparative Quantification of Health Risks, Vol. *1*; World Health Organization: Geneva, Switzerland, 2004.
(50) Mathers, C. D.; Loncar, D. Projections of global mortality and burden of disease from 2002 to 2030. *PLoS Med.* **2006**, *3*, e442.
(51) Grimm, N. B.; Faeth, S. H.; Golubiewski, N. E.; Redman, C. L.; Wu, J.; Bai, X.; Briggs, J. M. Global change and the ecology of cities. *Science* **2008**, *319*, 756−760.

DOI: 10.1021/acs.est.5b00873
Environ. Sci. Technol. 2015, 49, 4335−4344